

Second Edition

ENCYCLOPEDIA OF
**ATMOSPHERIC
SCIENCES**

Edited by

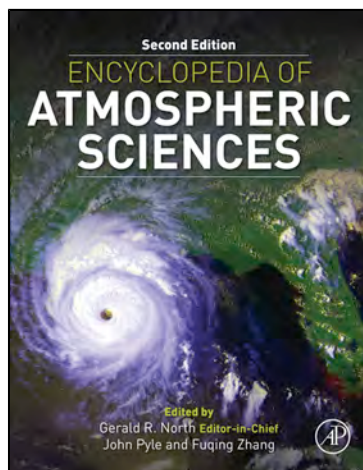
Gerald R. North **Editor-in-Chief**

John Pyle and Fuqing Zhang



**Provided for non-commercial research and educational use only.
Not for reproduction, distribution or commercial use.**

This article was originally published in the book *Encyclopedia of Atmospheric Sciences*, 2nd edition. The copy attached is provided by Elsevier for the author's benefit and for the benefit of the author's institution, for non-commercial research, and educational use. This includes without limitation use in instruction at your institution, distribution to specific colleagues, and providing a copy to your institution's administrator.



All other uses, reproduction and distribution, including without limitation commercial reprints, selling or licensing copies or access, or posting on open internet sites, your personal or institution's website or repository, are prohibited. For exceptions, permission may be sought for such use through Elsevier's permissions site at:
<http://www.elsevier.com/locate/permissionusematerial>

From Nigam, S., Baxter, S., 2015. Teleconnections. In: Gerald R. North (editor-in-chief), John Pyle and Fuqing Zhang (editors). *Encyclopedia of Atmospheric Sciences*, 2nd edition, Vol 3, pp. 90–109.

ISBN: 9780123822253

Copyright © 2015 Elsevier Ltd. unless otherwise stated. All rights reserved.
Academic Press

Teleconnections

S Nigam and S Baxter, University of Maryland, College Park, MD, USA

© 2015 Elsevier Ltd. All rights reserved.

This article is a revision of the previous edition article by S Nigam, volume 6, pp 2243–2269, © 2003, Elsevier Ltd.

Synopsis

Teleconnections refer to the climate variability links between non-contiguous geographic regions. Teleconnection patterns are extracted from analysis of the sea-level/tropospheric pressure variations on monthly (and weekly) timescales. The methods used in extraction of teleconnection patterns are discussed and applied to recent period data. Teleconnections are especially well-developed in Northern winter, when they strongly influence subseasonal variability, notably, in surface temperature and precipitation; the stratospheric and SST links are also noted. The patterns in boreal summer are shown, as are Southern Hemisphere teleconnections. Aspects of tropical–extratropical teleconnections are discussed, along with the relationship between annular modes and teleconnections. Finally, a teleconnection analysis with pentad (5-day averaged) data is presented to initiate discussion of teleconnection evolution.

Introduction

The term teleconnection is often used in atmospheric sciences to describe the climate links between geographically separated regions. The remote region need not exhibit fluctuations of the same sign in order to be ‘teleconnected.’ In fact, the interesting teleconnections often involve contemporaneous variations of opposite signs. Climate analysis is facilitated by the construction of a teleconnection map, which describes the linkage between a region of interest (a base point) and all other points in the domain that are farther than the decorrelation length scale of the variable. Teleconnection maps thus provide information about the structure of recurrent climate variability, especially its correlation-at-a-distance features. The maps are useful because climate variability is often manifest with such structure: for example, winter variations in temperature and rainfall over southern Europe and the Iberian Peninsula are frequently opposite to those over northwestern Europe and Scandinavia.

Teleconnection maps were first constructed for meteorological parameters measured at the Earth’s surface, such as the atmospheric pressure. The selection of the base point is a critical first step, and was, historically, guided by the investigator’s insights and interests. Today, base points can be selected more objectively, and the robustness of teleconnection maps can be ascertained by independent analyses. The statistical correlation of the fluctuations provides a measure of the teleconnection strength. The structure and strength of the teleconnection patterns change with season, altitude, choice of variable, and even temporal averaging of data. There are interesting differences between the hemispheres too, in part, due to the presence of extensive continents and mountainous zones in the Northern Hemisphere (NH). Teleconnectivity in the NH winter circulation has been extensively analyzed as teleconnections account for a significant portion of the winter variance in this region.

Climate teleconnections are present in observations that have been averaged in time over a period that is long enough to suppress the day-to-day weather fluctuations, but short enough to retain the seasonal-to-interannual component of climate variability. Although teleconnection patterns often evolve on submonthly timescales (~weeks), their spatial patterns are characterized in monthly and seasonal data. Monthly averages

are typically used since a month is longer than the period of most large-scale synoptic waves in the troposphere. Climate teleconnections thus highlight the ‘standing’ component of low-frequency variability – one with geographically fixed nodes and antinodes. The connectivity of remote regions manifest in the teleconnection map indicates the potential significance of remote forcing in the generation of regional climate anomalies. A teleconnection map based on contemporaneous correlations however cannot, by itself, discriminate between the forcing and response regions.

Although the structure of the prominent teleconnection patterns has been known for some time, the reasons for their origin are not yet well understood. For example, the mechanisms that excite and sustain the North Atlantic Oscillation (NAO) – one of the notable and earliest discovered patterns – are still being investigated. In the context of such investigations, it has been questioned if the teleconnection patterns that are typically regional (e.g., NAO), robustly portray the spatial structure of variability from the viewpoint of elucidation of the underlying dynamical processes.

Such concerns are relevant since the canonical teleconnection patterns typically represent the mature phase of variability. The mature-phase pattern, however, need not resemble the nascent-phase structure, which may be more revealing of the excitation mechanism. Identification of the evolution process from analysis of the mature-phase structure is thus difficult. The spatial imprint of variability captured by a teleconnection pattern can also be ineffective in revealing the underlying mechanisms if the region in question is the locus of two temporally independent physical and/or dynamical processes. While cautionary, these remarks do not call for a radically new analysis paradigm. Instead, they point to the need for more comprehensive analysis of variability, particularly, in the spatiotemporal domain, to facilitate insights into the evolutionary process. While in-depth analysis of this kind is beyond the scope of this article, it is important to let the reader know that contemporary teleconnection research is rooted in spatiotemporal analyses.

Additionally, while teleconnectivity has historically been identified from assessment of the correlation between some defined base point and distant points in the domain, not all

teleconnection patterns are uncovered from such analysis. Examples on subseasonal to seasonal timescales include the Madden–Julian Oscillation (MJO) and the annular modes, both of which are briefly discussed in subsequent sections. An example on interannual timescales is the El Niño–Southern Oscillation (ENSO), which impacts climate around the globe.

Analysis Method

Teleconnection patterns can be extracted from correlation analysis and from the calculation of principal components (PCs), among other techniques. Both methods have been widely used in climate research, and each offers some advantages.

Correlation

Correlation analysis is the more straightforward of the two methods. Consider a meteorological field such as geopotential height that denotes the height of an isobaric surface in the atmosphere. Geopotential height, ϕ , is a function of longitude and latitude, and assume that it is defined at M grid points; ϕ_i represents height at the i th longitude–latitude grid point. Geopotential height is also a function of time, and its monthly mean value is assumed to be available for several winters (N winter months). Interest in the variability of climate leads to the consideration of departures of monthly mean heights from their calendar month climatologies, with prime (') denoting the departures; $\phi'_{i,k}$ representing the height departure at the i th grid point in the k th month. The correlation in height departures at two grid points, i and j , is denoted by H_{ij} , and defined as

$$H_{ij} = \frac{\sum_{k=1}^N \phi'_{i,k} \phi'_{j,k}}{\left(\sum_{k=1}^N \phi'^2_{i,k}\right)^{1/2} \left(\sum_{k=1}^N \phi'^2_{j,k}\right)^{1/2}}$$

Knowledge of the correlation matrix, \mathbf{H} , can be used to construct a teleconnectivity map (\mathbf{T}) that objectively identifies the base points associated with various teleconnection patterns. The map is constructed by associating the magnitude of the strongest negative correlation between a grid point and all others with that grid point, i.e., $T_i = |\text{most negative member in the } i\text{th row of the correlation matrix } \mathbf{H}|$. The local maxima in this map (\mathbf{T}) identify the potential base points. Linkage between the neighboring base points is assessed by examining the sites of their strongest negative correlations. A cluster of linked base points constitutes the core of the teleconnection pattern, and three prominent patterns are identifiable using this technique.

Teleconnection Map

Climate teleconnections were first investigated in the sea-level pressure (SLP) field. SLP is however an ill-defined quantity over land, particularly near the mountains; it can moreover be influenced by local meteorological processes. Teleconnectivity is thus better analyzed in upper-air data, which became available since the mid to late 1940s. The preferred analysis variable in recent decades has been the geopotential height – a measured quantity, whose horizontal and vertical gradients are proportional to the wind and temperature, respectively. Northern winter is the preferred season for teleconnection

analysis in view of the pronounced climatological stationary waves (from impressive mountains and continents in the NH) that impart a significant ‘standing’ component to the interannual fluctuations.

Figure 1(a) shows the teleconnectivity in the 500-mb geopotential height field during Northern winter. The map is constructed from correlation analysis of December, January, and February (DJF) height anomalies from 0 to 90° N for the 1979–2008 period; the data are from NOAA’s Climate Forecast System Reanalysis (CFSR). This recent reanalysis takes advantage of the latest advances in data assimilation and incorporates important data from the satellite era, and thus only extends back to 1979. This figure is comparable to Figure 7(b) in the pioneering study by Wallace and Gutzler (1981). It identifies three major teleconnection patterns in the NH: the NAO, the North Pacific Oscillation/West Pacific pattern (NPO/WP), and the Pacific–North America (PNA) pattern. The NAO and NPO/WP each consist of two base points over the Atlantic and Pacific basins, respectively. The PNA, as identified by Wallace and Gutzler (1981), consists of four base points: the subtropical Pacific near the dateline, the Aleutians, interior northwestern North America, and the southeastern United States. Note, however, that the fourth base point over southeastern United States is missing in Figure 1(a).

This brings to light an issue regarding the stability of teleconnection patterns. Changing the domain and time period of the analysis can introduce some differences: Besides the missing PNA center, there are other differences between the seminal analysis of Wallace and Gutzler and Figure 1(a). The NAO-related pattern exhibits a noticeable eastward shift, as does the third PNA center. Note, data set differences are unlikely to be the origin as the large-scale rotational flow is similarly represented in atmospheric data sets. While notable, the teleconnectivity differences are viewed as modest considering the nonoverlapping periods of the two analyses. This assessment is supported by Figure 1(b), which shows the teleconnectivity map from a similar analysis of longer period data (1949–2009), one encompassing the previous nonoverlapping periods. While the NAO centers and the third PNA center here are more in accord with the Wallace and Gutzler analysis, the fourth PNA center remains indiscernible. Interestingly, the NPO/WP centers of action are also not identifiable in the longer period analysis. Even so, the overall structure of the teleconnectivity map is similar in Figure 1(a).

The correlation analysis reveals the base points of a teleconnection pattern. An index constructed using the magnitude of fluctuations at the base points is used to track the pattern amplitude. For example, the PNA index is defined as

$$\alpha_{\text{PNA}}(k) = \frac{1}{3} \left(\frac{\phi'_{A,k}}{S_A} - \frac{\phi'_{B,k}}{S_B} + \frac{\phi'_{C,k}}{S_C} \right)$$

where A, B, and C are the marked base points of the PNA pattern (Figure 1(a)). S_i in the above definition denotes the standard deviation of height anomalies at the i th base point. Likewise an index can be constructed for the NAO- and NPO/WP-related patterns, using two base points in each case.

Correlation analysis is a physically intuitive and objective method for identifying climate teleconnections but the obtained patterns may not be independent, especially, if spatial

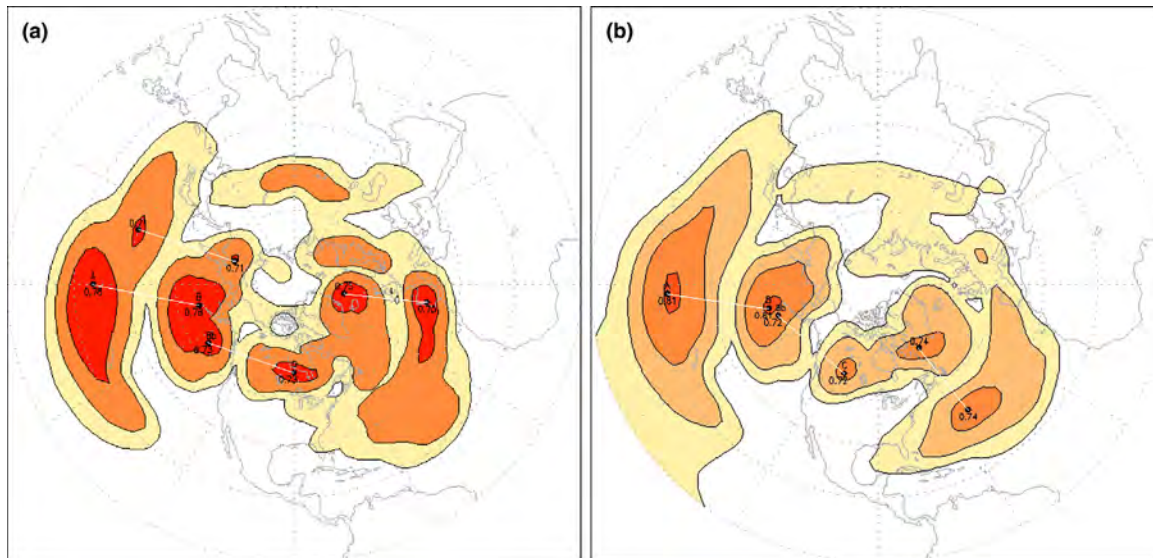


Figure 1 (a) 500-mb geopotential height teleconnectivity map for Northern Hemisphere winter (DJF), comparable to seminal **Figure 7(b)** in Wallace, J.M., Gutzler, D.S., 1981. Teleconnections in the geopotential height field during the northern hemisphere winter. *Mon. Weather Rev.* 109, 784–812. Contour/shading starts at a correlation of 0.5 and increases at 0.1 intervals. Points A, B, Bb, and C refer to the centers of actions of the PNA pattern. Points B and Bb are generally associated with the Aleutian Low center of action. (b) 500-mb geopotential height teleconnectivity map for Northern Hemisphere winter (DJF), comparable to seminal **Figure 7(b)** in Wallace, J.M., Gutzler, D.S., 1981. Teleconnections in the geopotential height field during the northern hemisphere winter. *Mon. Weather Rev.* 109, 784–812. **Figure 1**, except for a prolonged analysis period from 1949 to 2009. Contour/shading starts at a correlation of 0.5 and increases at 0.1 intervals. Points A, B, Bb, and C refer to the centers of actions of the PNA pattern. Points B and Bb are generally associated with the Aleutian Low center of action. DJF, December, January, February.

structures overlap. This, for instance, is the case in the Pacific, where three prominent patterns – PNA, WP/NPO, and the ENSO response (shown later) – overlap to varying extent in the extratropical sector. Not surprisingly, the correlation method proved unsuccessful in capturing the ENSO response in the extratropics as a teleconnection pattern. Could this be a consequence of focusing on analysis of midtropospheric variability? The 500-hPa level – a level of near-zero divergence – is, perhaps, not the level of choice for identifying tropical–extratropical interactions instigated by deep convective heating in the Tropics. Horizontal divergence associated with deep convection, such as during El Niño winters, is usually strongest in the tropical upper troposphere (~ 200 hPa). The associated midlatitude response, on the other hand, is quasi-geostrophic in character, and hence approximately nondivergent. Tropical–extratropical interactions are thus best diagnosed at a pressure level that captures the divergent outflow in the Tropics and that is near a nondivergent level in the extratropics. The 200-hPa level meets these criteria to a large extent.

Repeating the correlation analysis of height fluctuations at 200 hPa did not yield any new information on teleconnectivity. In particular, no new base points were identified and the ENSO response in the extratropics remained unidentified as before.

Principal Component Analysis

Principal component analysis (PCA) is an elegant and widely used method for determining the structure of recurrent variability. A common name for it is empirical orthogonal function (EOF) analysis. This method also analyzes the structure of the correlation matrix – the covariance matrix is preferred, though –

but focuses on regions that account for a substantial portion of the temporal variance rather than just those which exhibit strong negative correlations with distant points in the domain. In contrast with the previous method, the technique yields both the spatial patterns of recurrent variability and the extent to which these are present, or projected, in the observed anomaly record. The projection, or amplitude, is called the PC while the spatial pattern is referred to as the loading vector (LV) in the technical literature.

Recurrent variability patterns identified from PCA are spatially and temporally independent, or orthogonal. Such relationship among patterns is often helpful in investigating the origin and governing mechanisms of variability but can be relaxed in one of the dimensions – space or time – if the orthogonality constraints prove restrictive. For example, it is conceivable for two temporally independent variability patterns to have overlapping spatial structure. Imposition of temporal and spatial orthogonality constraints in this case may not lead to a physically meaningful analysis.

The EOF analysis results in a series of spatial patterns, or LVs, each one explaining successively smaller portion of the total temporal variance. One can view these recurrent patterns as teleconnection patterns. The pattern amplitude is given by the time-dependent PC. The anomaly record can be reconstructed by summing the product of the spatial patterns (LVs) and their PCs.

Rotated Principal Component Analysis

PCA provides an efficient and unique characterization of recurrent variability in terms of a small number of uncorrelated spatial patterns. The patterns are chosen so that each one

successively explains the maximal residual variance in the anomaly data set. For instance, the leading PC is obtained by requiring that it maximizes the sum of the squared temporal correlation between itself and the anomaly time series at all spatial points in the domain. The resulting PCs are temporally orthogonal while the LVs are spatially orthogonal. Spatial orthogonality can however be restrictive and, in many cases, undesirable, as discussed earlier: Although the leading LV is not directly impacted, subsequent LVs are often constrained to have predictable geometric relationships vis-a-vis the leading pattern; domain geometry, thus, becomes an influencing factor, itself.

For these and other reasons, a variant of PCA, called the rotated principal component analysis (RPCA), has become popular since it yields patterns that are no longer constrained to be spatially orthogonal; domain geometry is thus much less influential; rotated PCs continue to be temporally orthogonal, though. The linear transformation (or solid rotation) of PCs that is widely used in meteorology is called the 'varimax' rotation. It is determined by the requirement that the variance of the squared correlations between each rotated PC and the original time series be maximized. Focusing on the variance, rather than sum (as in unrotated analysis), of the squared correlations increases spatial discrimination, and facilitates interpretation of the obtained patterns.

Typically, only a subset of the leading PCs is rotated. Although several criteria exist to guide the choice of this subset, the sensitivity of results to the rotated number offers good practical guidance. In most meteorological applications, 8–10 of the leading PCs are rotated; in most applications reported here, the number is eight.

A more technical discussion of RPCA can be found in Barnston and Livezey where RPCA is advanced as a preeminent method for defining and monitoring of teleconnection patterns.

Empirical Orthogonal Teleconnection

An alternate method for identifying the teleconnection patterns is empirical orthogonal teleconnection (EOT) analysis, developed by Van den Dool et al. (2000) EOT analysis is conducted by finding a base point in the domain that explains the most variance at all the other points combined, using linear regressions. This leading spatial pattern is defined from the linear regression coefficients of this base point, while its time series is simply the raw time series at the base point. Subsequent patterns are obtained by repeating this procedure on a reduced data set, from which the first pattern has been linearly removed.

The analysis results in a series of spatial patterns, or EOTs, that are not constrained to be spatially orthogonal, but whose time series are independent. In this way, it is similar to RPCA. Other than the inherent simplicity, EOT analysis holds another advantage over RPCA: In RPCA, only a small subset of PCs are subject to rotation; no such truncation is required in EOT analysis.

Northern Winter Teleconnections from RPCA

The leading patterns of recurrent height variability are extracted from RPCA and shown in Figure 2. The DJF anomalies during 1979–2008 winters were analyzed in the 30° S–90° N domain. Analysis was conducted at the 200-hPa level in order to also

capture the tropical–extratropical interactions (e.g., ENSO related) that are prominently manifest in the upper troposphere, for reasons stated earlier. Height anomalies were multiplied by the square root of the cosine of latitude to achieve grid-area parity, which prevents polar regions with many more points on a regular latitude–longitude grid, from unduly influencing the analysis. The covariance, rather than correlation, matrix was analyzed so that regions with large variance can exert greater control on the analysis outcome. The eight leading PCs were rotated using the varimax criterion. The PCs are normalized and dimensionless and the spatial patterns (LVs) show nothing but the regression of the PCs onto the 200-mb height field.

The leading pattern explains ~15% of the monthly variance in the domain, with two centers of action in the Atlantic sector. Note the spatial similarity to the Atlantic Basin teleconnectivity structure in Figure 1, sans its earlier noted eastward shift. This leading pattern is clearly the NAO. Its structure is consistent with its historical characterization as a north–south dipole in SLP that represents out-of-phase fluctuations of the Icelandic Low and Azores High. For example, Hurrell's monthly NAO index is constructed from the difference of normalized SLP anomalies at Ponta Delgada, Azores and Stykkisholmur, Iceland; the NAO pattern depicted in Figure 2 is thus in its positive phase, which strengthens the regional winter circulation features. The identification of NAO as the leading pattern in the 200hPa analysis is important both for explanation of regional variance and for showing NAO variability to be temporally orthogonal to the other NH variability patterns. The NAO pattern is manifest on timescales ranging from subseasonal to decadal, as seen in Figure 3. The NAO pattern is closely linked with meridional excursions of the Atlantic jet, and related storm track displacements; northward in the positive phase of the pattern.

The second, third, and fourth leading patterns all have centers of action in the Pacific sector, attesting to RPCA's skill in separating overlapping variability structures. The second leading pattern represents higher geopotential heights in all sectors of the northern subtropics, but especially over the central/eastern Pacific. Higher upper-level heights are typically associated with a warmer air column underneath, since the atmosphere is in hydrostatic balance. The pattern of variability is thus associated with a warming of the Tropics, such as during El Niño winters. The presence of a subtropical ridge to the southeast of the Hawaiian Islands is indicative of linkage with ENSO, for deep convection in this tropical Pacific sector and the related divergent outflow are linked with the development of an upper-level anticyclonic circulation in the subtropics. The subtropical ridge also reflects the southeastward extension of the Asian-Pacific jet in El Niño winters. The ENSO pattern is also characterized by an east–west dipole near North America with a negative anomaly along and off the west coast and a positive anomaly near the south shore of Hudson Bay.

The PC associated with this spatial pattern exhibits inter-annual variability and is correlated ($r = 0.6$) with the Niño 3.4 index, which is the average sea surface temperature (SST) anomaly in the central-eastern equatorial Pacific (5° S–5° N, 170–120° W) and operationally used to define the state of ENSO. While this pattern, which explains ~13% of the monthly winter variance, is characterized as the ENSO response, the related PC exhibits some long-term trend as well.

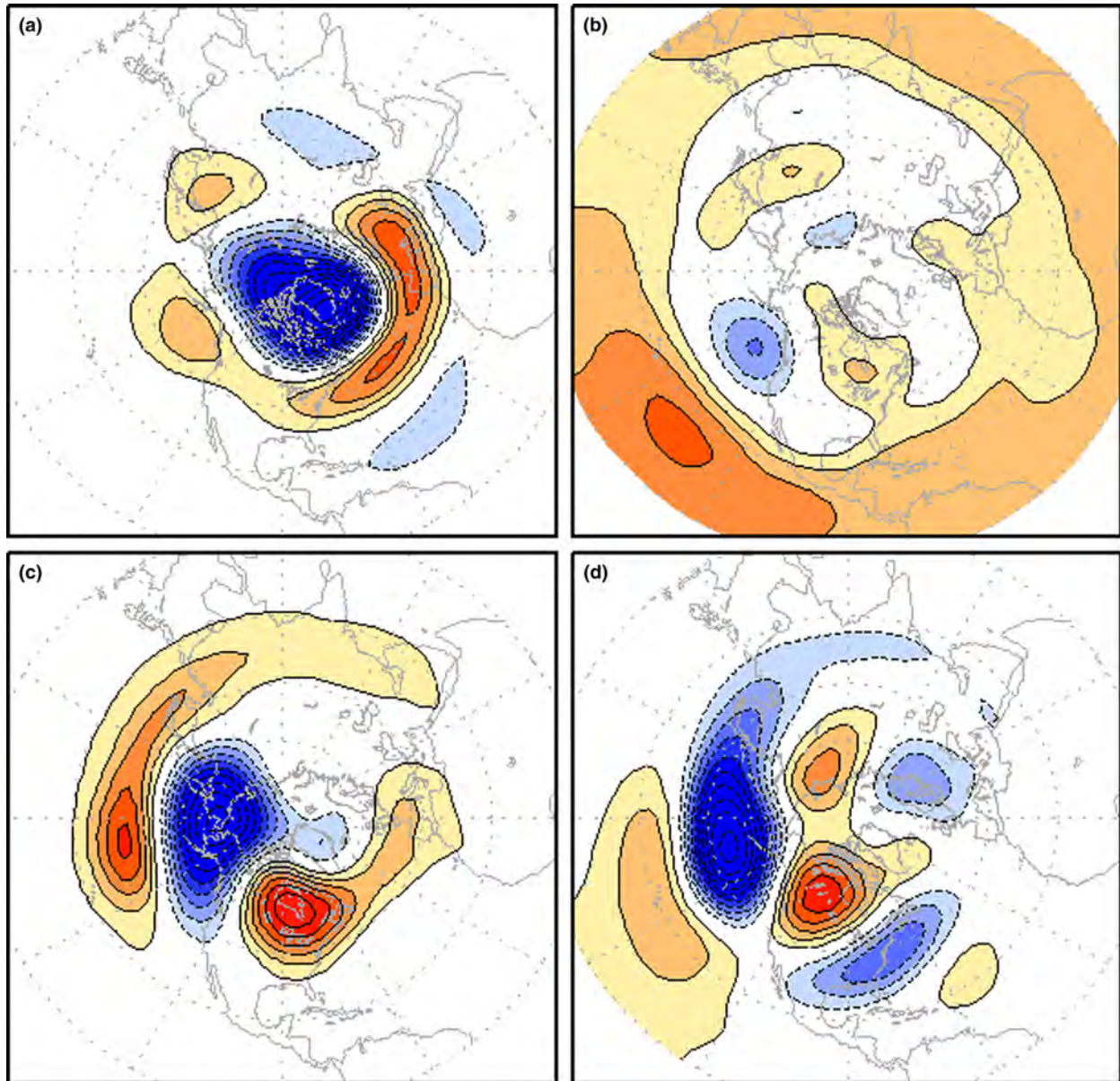


Figure 2 The four leading teleconnection patterns from a rotated EOF analysis conducted on monthly 200-mb wintertime height anomalies: (a) NAO, (b) ENSO related, (c) NPO/WP, and (d) PNA. The domain of the analysis is 30° S– 90° N. Contour/shading interval is 10 m; the zero contour is suppressed. Percentage of explained variance: (a) 14.6, (b) 12.5, (c) 11.4, (d) 11.1. NAO, North Atlantic Oscillation; ENSO, El Niño–Southern Oscillation; NPO/WP, North Pacific Oscillation/West Pacific; PNA, Pacific–North America.

It is remarkable that RPCA of upper-tropospheric heights can identify the ENSO-related height pattern without any reference to the underlying SST variability. Note that teleconnection analysis of the 200-hPa height variability in the same period was unsuccessful in this regard.

The third and fourth leading patterns of Northern winter height variability each explain $\sim 11\%$ of the monthly variance. The third leading pattern in **Figure 2** consists of a north–south dipole in the North Pacific with a downstream height anomaly over eastern North America centered over Hudson Bay. This pattern is referred to as the NPO/WP pattern as the related SLP pattern (shown later) closely resembles the NPO, a recurrent subseasonal variability pattern in SLP, first identified by Walker

and Bliss in 1932. The ‘West Pacific’ part of the name is from Wallace and Gutzler’s teleconnection analysis of 500-hPa heights. The NPO/WP pattern can be viewed as the NAO analog in the Pacific Basin: both patterns describe subseasonal height fluctuations in the jet-exit regions of the climatological jets streams. The fluctuations have a meridional dipole structure with a stronger polar center in both cases, and linked with meridional displacements of the jets and related storm tracks. A multivariate description of the NPO/WP pattern and its similarity with the NAO can be found in Linkin and Nigam.

The fourth leading pattern is the PNA, defined by the coherent arcing pattern of height fluctuations of alternating signs, beginning with the center over Hawaii and followed by

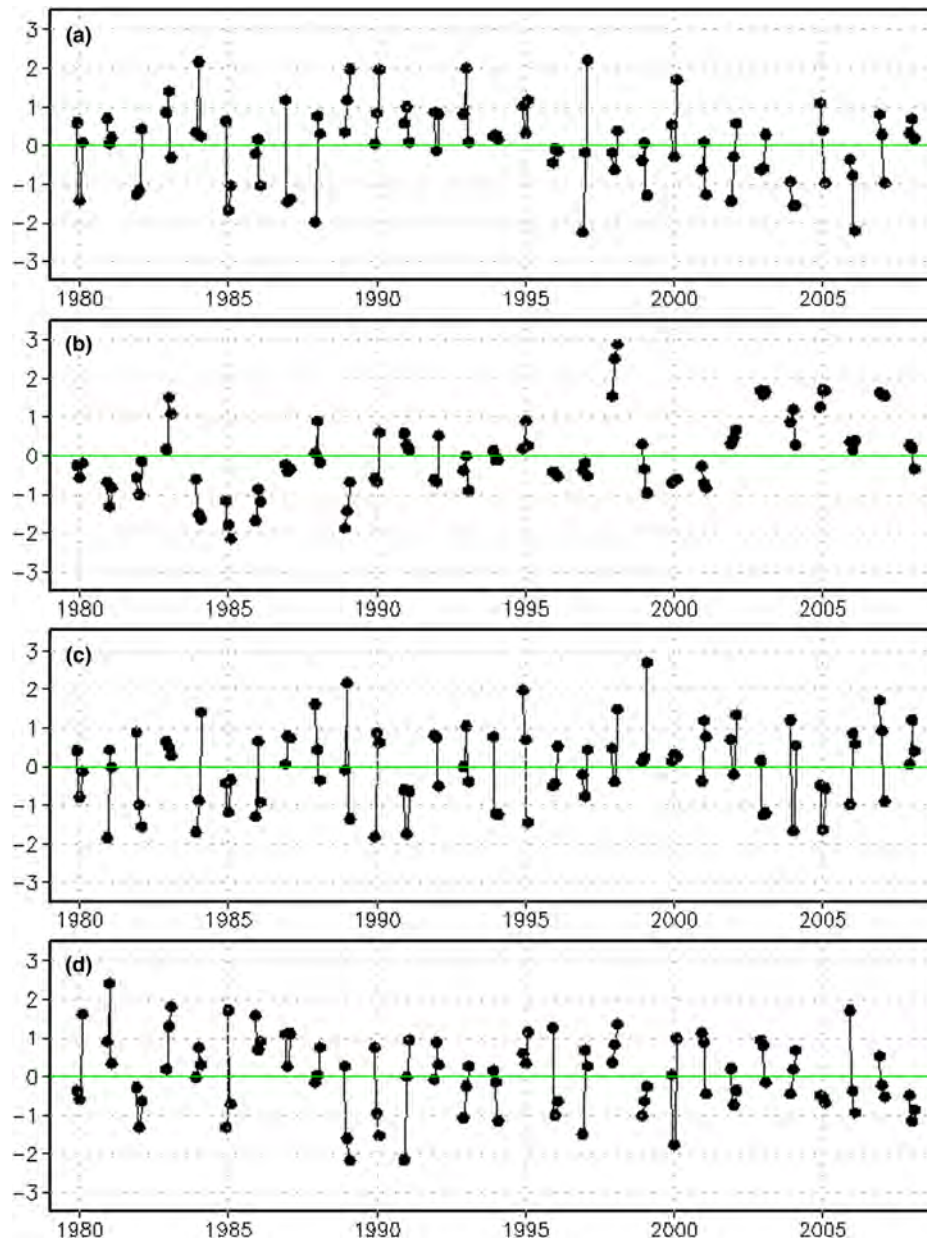


Figure 3 The principal component time series for each pattern is shown. (a) NAO, (b) ENSO related, (c) NPO/WP, (d) PNA. Note that there are only values for the DJF season. NAO, North Atlantic Oscillation; ENSO, El Niño-Southern Oscillation; NPO/WP, North Pacific Oscillation/West Pacific; PNA, Pacific–North America.

centers over the tip of the Aleutians, northwestern North America, and Southeast United States. In the positive phase (depicted), the pattern consists of positive height anomalies over northwestern North America. In the Pacific sector, the height anomalies represent eastward displacement and meridional focusing of the Asian-Pacific jet. It is interesting to note the position of the subtropical ridge in the PNA- and ENSO-related patterns, as this is helpful in pattern identification: The ridge is over the Hawaiian Islands in the former but southeastward of Islands in the latter. The variability timescales of the patterns are also distinct: subseasonal and interannual, respectively (Figure 3). The separation of the PNA- and ENSO-related patterns is important as PNA was

once viewed as the extratropical response of ENSO. The PNA and NPO/WP patterns are also distinct, notwithstanding the broadly similar structure over the North Pacific–North American region; closer inspection reveals the two patterns to be in spatial quadrature in this sector; for example, the NPO/WP trough tracks the North American coastline, which is a nodal line in the PNA pattern.

Surface Temperature and Precipitation Impacts

Teleconnection patterns are of considerable interest because of their impact on surface hydroclimate. Significant climate anomalies on subseasonal-to-interannual timescales are often

attributable to a dominant phase of one or more teleconnection patterns. Figure 4 shows the SLP, surface temperature, and precipitation footprints of the NAO. The temperature and precipitation data sets used in this analysis are from the Climate Research Unit (CRU) of the University of East Anglia, namely the TS 3.1 climate database. The SLP pattern bears striking resemblance to the 200-hPa height pattern (Figure 2(a)), indicating an equivalent barotropic vertical structure. The strongest impacts of the NAO emerge over Europe and North Africa. The NAO results in nearly all of Europe experiencing above-normal temperatures, while cooler temperatures prevail from Saharan Africa east-northeastward to the eastern Mediterranean, Middle East, and the Arabian Peninsula. The temperature pattern at the surface results largely from advection of climatological temperature by the NAO circulation (i.e., $-V_{\text{NAO}} \cdot \text{Grad}(T_{\text{CLIM}})$); for example, cooler temperatures over Africa arise from the cold advection by

northeasterlies tracking the eastern flank of the high SLP cell. Correlation coefficients are shown in Figure 4 to indicate the significance of the impact, although they conceal the fact that temperature anomalies over Europe are larger than those over Africa. The precipitation pattern likewise shows a wet-dry dipole with northern Europe experiencing above-normal, and the Iberian Peninsula and southern Europe below-normal precipitation. This impact is not obvious from the geopotential and SLP patterns unless the impact of NAO on the jet stream, and thus storm tracks, is considered. In the depicted positive phase, NAO results in enhanced zonal wind north of the Azores center and reduced zonal wind to the south. The northward displaced jet stream and storm track account, in part, for the observed precipitation dipole.

The NAO influences the surface climate of North America as well. A north-south dipole in temperature is again observed: cold in northeastern North America, warm to the south; both

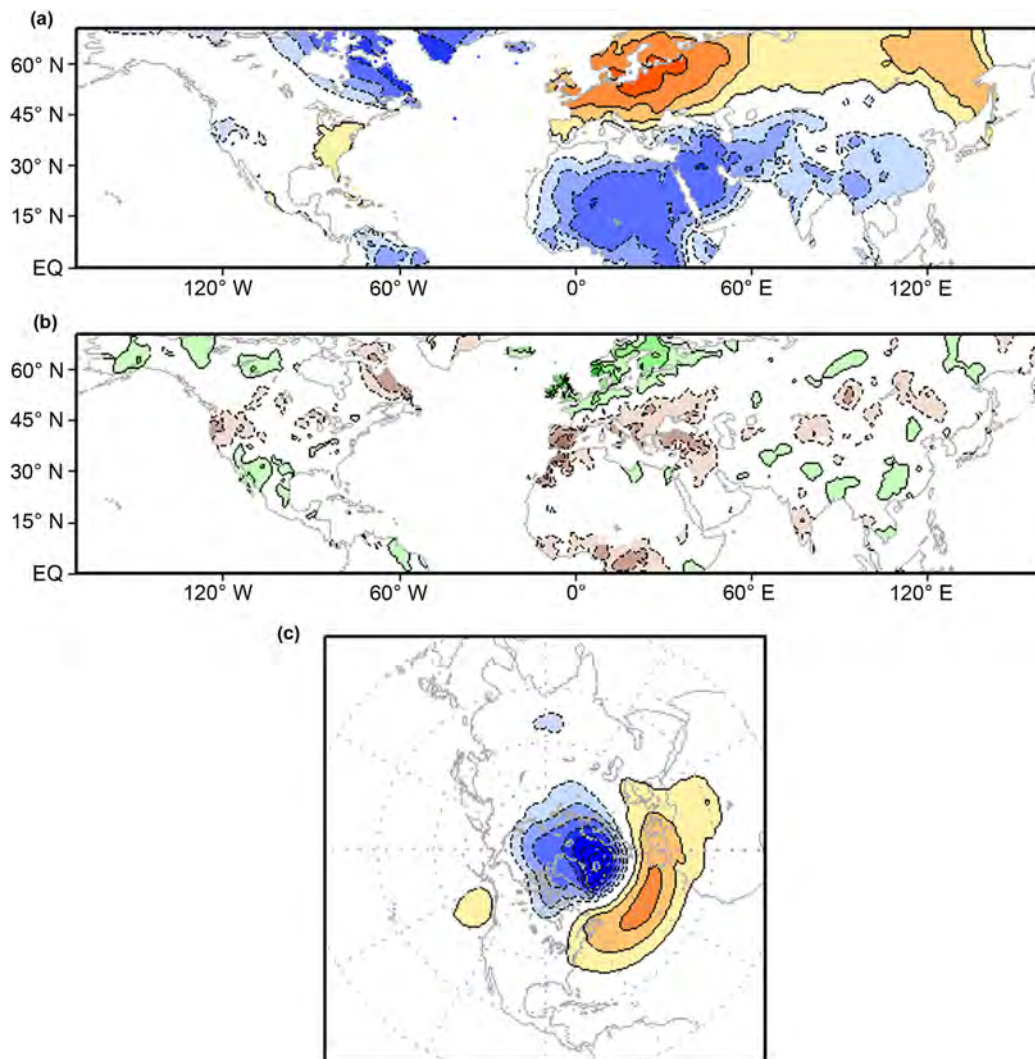


Figure 4 (a) Temperature, (b) precipitation, and (c) SLP footprints of the wintertime NAO pattern seen in Figure 2. Correlation between NAO principal component and CRU temperature and precipitation is contoured at 0.15 intervals; the zero contour is suppressed. For SLP the regression coefficient between the principal component and the SLP field from the CFSR is contoured at 1-hPa intervals, and the zero contour is suppressed. NAO, North Atlantic Oscillation; CFSR, Climate Forecast System Reanalysis.

consistent with the regional SLP signal. The precipitation impacts are less coherent and significant than in Europe, except along the west coast of the Labrador Sea and Davis Strait; the deficit here resulting from off-shore moisture advection by the NAO circulation. Interestingly, there is a significant dry anomaly on the central US West Coast that is associated with a weak ridge over the Gulf of Alaska (**Figure 2(a)**). This impact feature is revisited when annular modes are discussed.

The surface signatures of the ENSO-related pattern are shown in **Figure 5**. The SLP signature is notably weak and focused in the Gulf of Alaska. Unlike NAO where regional thermal advection shaped surface temperature, the significant ENSO-related warming of the global northern Tropics (at both lower and upper levels) results from the propagation of atmospheric waves instigated by ENSO-related diabatic heating changes over the tropical Pacific. There is also a tendency for warmer winters across much of North America, centered on the United States–Canadian border, along with northern Europe and East Asia. Precipitation impacts are also notable in the

deep Tropics, with drying in eastern South America and increased precipitation over eastern Africa. The ENSO-related pattern results in a southward shift of precipitation across North America with increased precipitation along the US West Coast and southern tier states. Equally noteworthy are the positive precipitation anomalies over the northern Indian subcontinent, including the Himalayas. It is important to note that **Figure 5** does not fully capture the canonical ENSO impact on winter hydroclimate (e.g., as defined from correlations of the Niño 3.4 SST index) but comes close in most regions.

The NPO/WP pattern results in significant modulation of the North American surface climate (**Figure 6**). The SLP pattern is robust and oriented much as the NAO's, reflecting similar variability mechanisms. The NPO/WP circulation in the lower troposphere leads to impressive temperature correlations (exceeding 0.5) over central-eastern North America from anomalous thermal advection and related meteorological feedbacks; see Linkin and Nigam for more information. Intrusion of the sub-Arctic air into the continental interior in

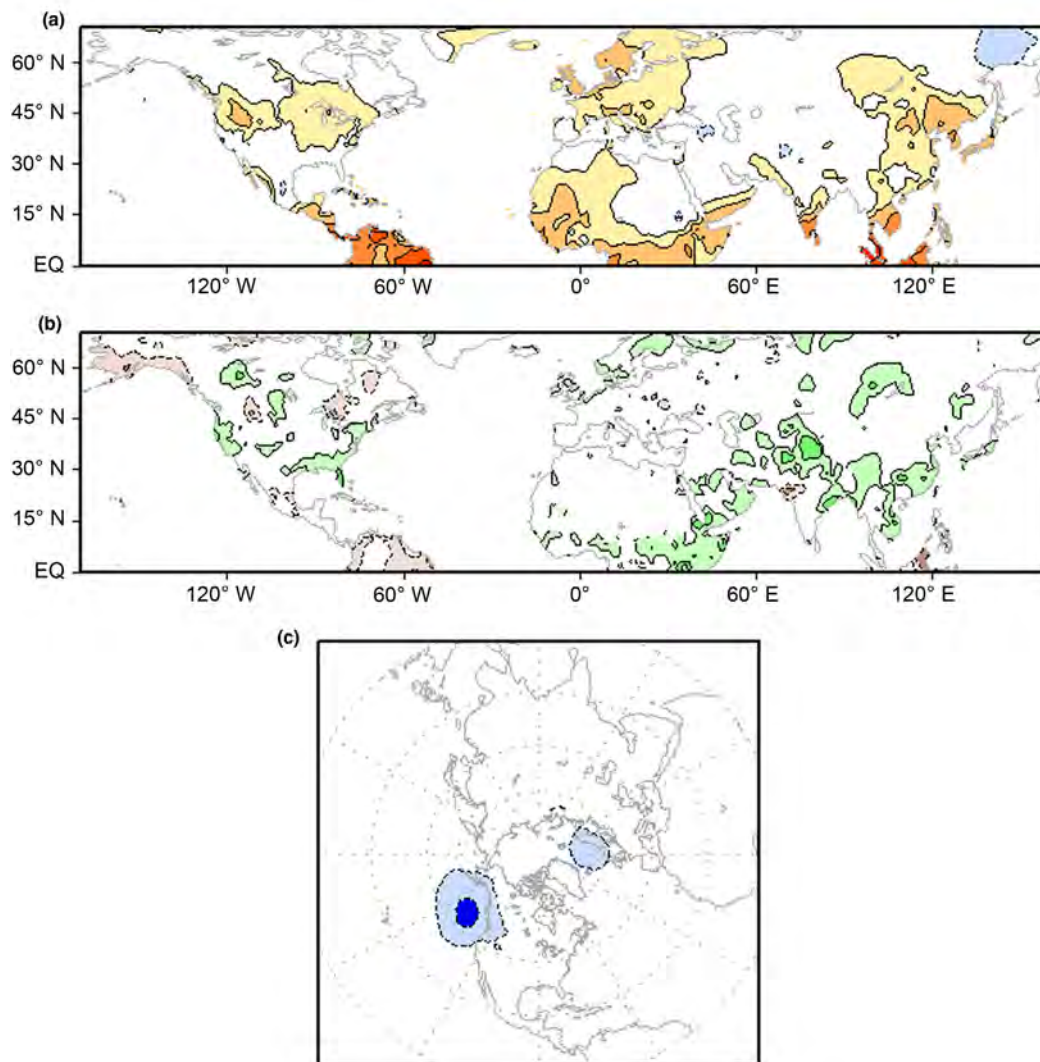


Figure 5 Same as in **Figure 3** except for ENSO pattern (a) temperature, (b) precipitation, (c) sea-level pressure. ENSO, El Niño–Southern Oscillation.

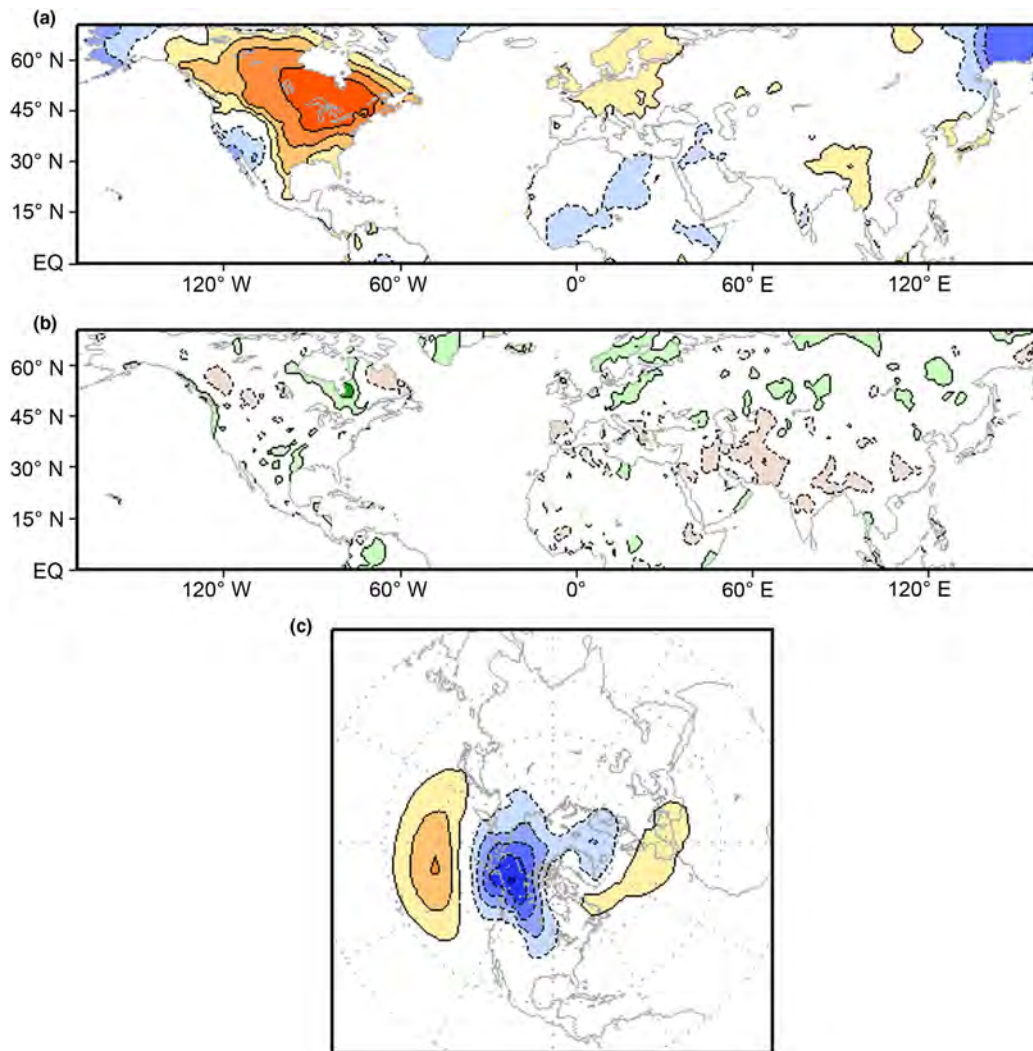


Figure 6 Same as in [Figure 3](#) except for the WP/NPO pattern (a) temperature, (b) precipitation, (c) sea-level pressure. WP/NPO, West Pacific/North Pacific Oscillation.

the negative NPO/WP phase (weakened Aleutian Low) leads to below-normal temperatures, especially to the east of the Rockies, for example. The high correlations suggest that between one-quarter and one-half of the monthly temperature variance in the core influence region is explainable by NPO/WP variability. The precipitation impact is weaker and the spatial pattern less coherent, but potentially important in the Pacific Northwest and southern Great Plains. Like the NAO, the NPO results in meridional perturbation of the jet stream in its exit region; since this occurs over the wide Pacific Basin, the related storm track modification is not manifest in analysis of continental precipitation.

The PNA pattern's influence on North American surface hydroclimate ([Figure 7](#)) is, perhaps, most impressive. The SLP footprint in the Bering Sea and Gulf of Alaska is ~ 6 hPa, larger than of the other Pacific Basin patterns, including ENSO. The temperature impact is characterized by a strong northwest–southeast dipole across North America. Not surprisingly, the impact is focused on Northwest

Canada and the Southeast United States, the third and fourth centers of action of the pattern, respectively; again, with anomalous thermal advection defining the large-scale impact structure, if not its amplitude. At first glance, the precipitation impact appears similar to the opposite phase of the ENSO-related pattern ([Figure 5\(b\)](#)). Closer inspection, however, reveals a subtle shift in the greatest precipitation correlation regions. The PNA response is defined by large correlations over interior eastern North America, centered on the Tennessee and Ohio Valleys and extending across the Great Lakes into Northern Canada. A similarly signed signal is evident in the Pacific Northwest and Alaska as well. The positive-phase PNA precipitation response ([Figure 7\(b\)](#)) thus consists of only deficits across the United States. The deficit over the eastern United States results from the southward displacement of the Atlantic jet and storm track that are linked to the circulation anomalies associated with the third and fourth centers of the PNA height pattern.

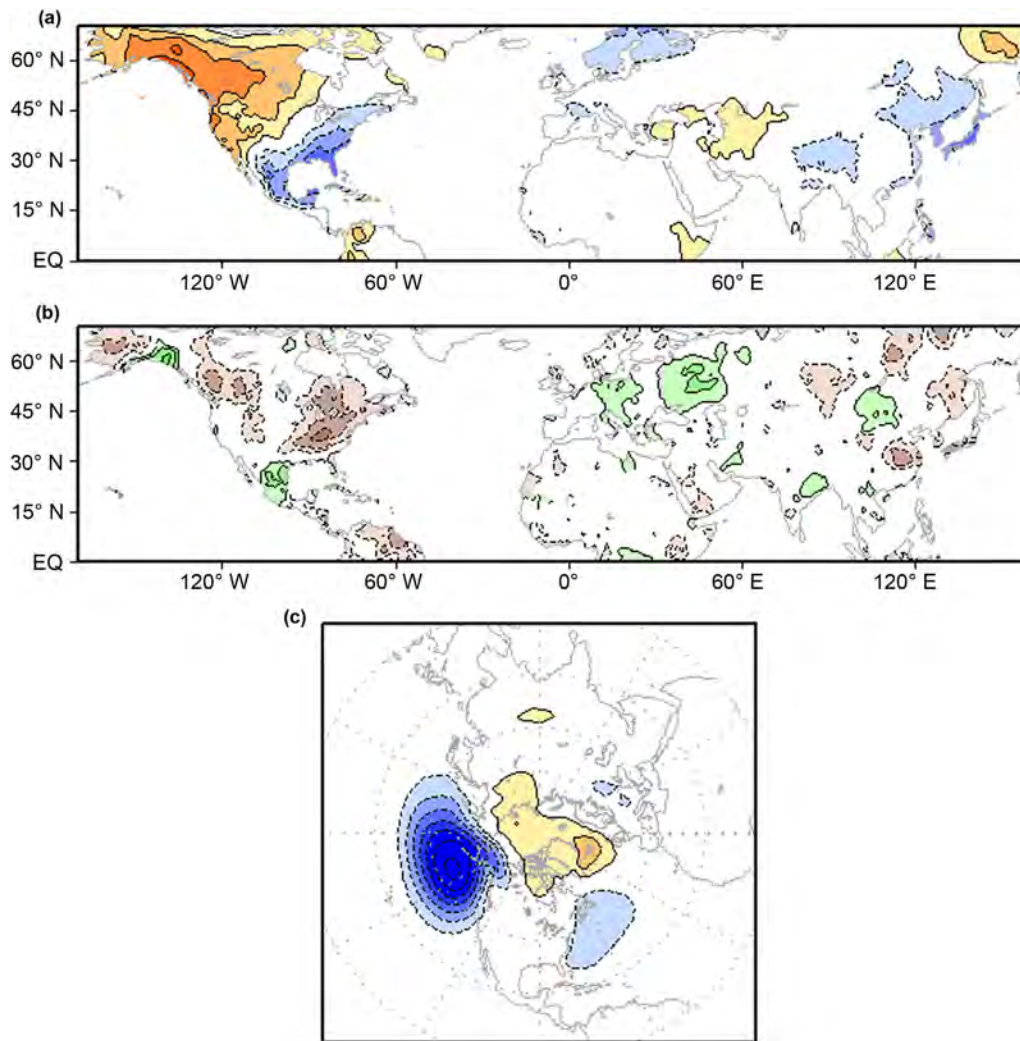


Figure 7 Same as in **Figure 3**, except for the PNA pattern (a) temperature, (b) precipitation, (c) sea-level pressure. PNA, Pacific–North America.

Stratospheric Signature

Teleconnection patterns are obtained from the analysis of connectivity of tropospheric climate variability. Understanding the mechanisms generating the remote response, i.e., teleconnectivity, in some cases warrants analysis of the related stratospheric links since stratospheric circulation can be an influence pathway between distant tropospheric regions. The enabling role of the stratosphere in generating aspects of tropospheric teleconnectivity is getting increasing attention in observational and modeling analyses. Two of the four tropospheric teleconnection patterns – NAO and NPO/WP – exhibit impressive stratospheric links (**Figure 8**). Not surprisingly, both involve meridional displacement of the subtropical jets, especially in the jet-exit sector. Such change in the tropospheric jet structure (a poleward shift in the positive NAO and NPO/WP phase) modulates the refractive index for the meridional-vertical propagation of planetary waves; a poleward jet shift, for instance, reduces the orographically forced stationary wave response in both the troposphere and stratosphere in dynamical models. Jet perturbations influence not only wave

propagation but also wave forcing; the latter by modulating flow over orography and regions of strong climatological vorticity gradients, for instance. The dynamical and thermodynamical mechanisms linking the troposphere and stratosphere are of great interest in modern climate studies.

Figure 8 shows the regressions of the NAO and NPO/WP PCs on geopotential heights at 100 hPa (~16 km), 50 hPa (~20 km), and 10 hPa (~30 km); the NAO ones are in the left column. The NAO footprint in the stratosphere is significantly annular, i.e., anomalies of one sign in the polar region surrounded by opposite-signed anomalies in the midlatitudes. The tropospheric structure is less annular, prompting some to view NAO as the regional expression of the annular mode of SLP; the annular modes are discussed in a later section. The NAO stratospheric structure can be broadly characterized as consisting of out-of-phase variations of the polar vortex and surrounding regions. The NPO/WP one, on the other hand, reflects displacement of this vortex into North America. This difference between displacement of the vortex and the breakdown or splitting of the vortex is analogous to the two distinct

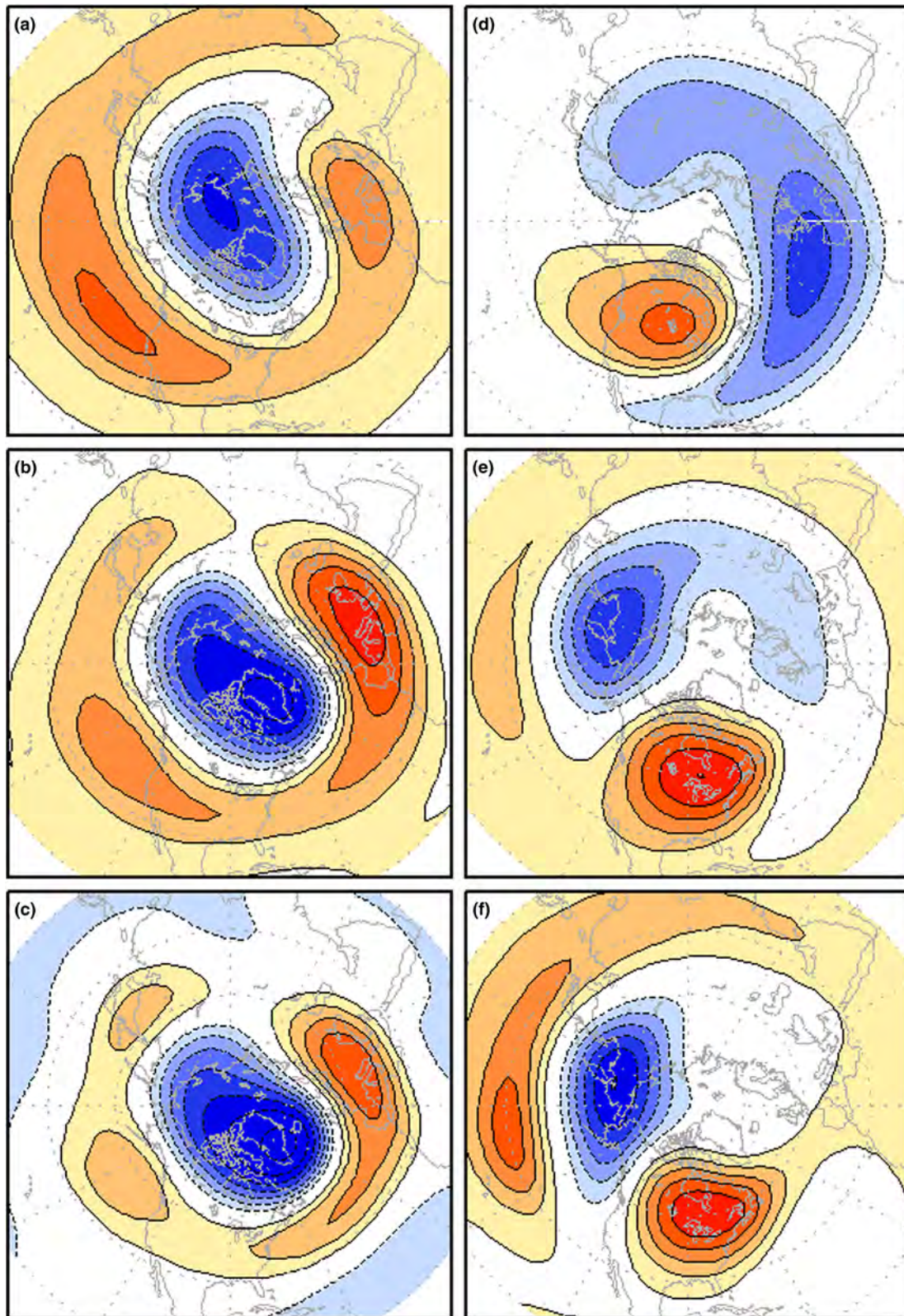


Figure 8 Stratospheric footprints of the two leading teleconnection patterns with substantial stratospheric signatures: (a)–(c) show the regression of the NAO PC onto 10-mb, 50-mb, and 100-mb normalized geopotential height anomalies, respectively. The contour interval is 0.2 standard deviations. The zero contour is suppressed in all cases. Panels (d)–(f) show the same except for the WP/NPO pattern. NAO, North Atlantic Oscillation; PC, principal component; WP/NPO, West Pacific/North Pacific Oscillation.

types of sudden warming events that occur in the stratosphere. In the case of a split vortex or complete breakdown of the vortex, an equivalent barotropic structure is observed as in the case of the NAO stratospheric signature. The NPO-related vortex displacement tends to be more baroclinic in nature, at least in the stratosphere, as evidenced by the westward tilt with height.

SST Anomalies

The teleconnections described above represent standing modes of atmospheric circulation variability on subseasonal-to-interannual timescales. As such, it is of interest to inquire

into the nature of related SST anomalies, which in the Pacific Basin can provide additional discrimination between the overlapping height variability patterns. Figure 9 shows the SST correlation of the four PCs. The NAO SST footprint reveals a characteristic tripole feature in the Atlantic Basin, with cooler temperatures underneath strengthened westerlies in the North Atlantic. SST anomalies associated with the NAO also appear in the extratropical Pacific that are only slightly weaker than in the Atlantic. It is noteworthy that NAO variability is not correlated with tropical Pacific SSTs, at least contemporaneously during Northern winter months. Herein lies a great dilemma that serves as the basis for a significant portion of contemporary

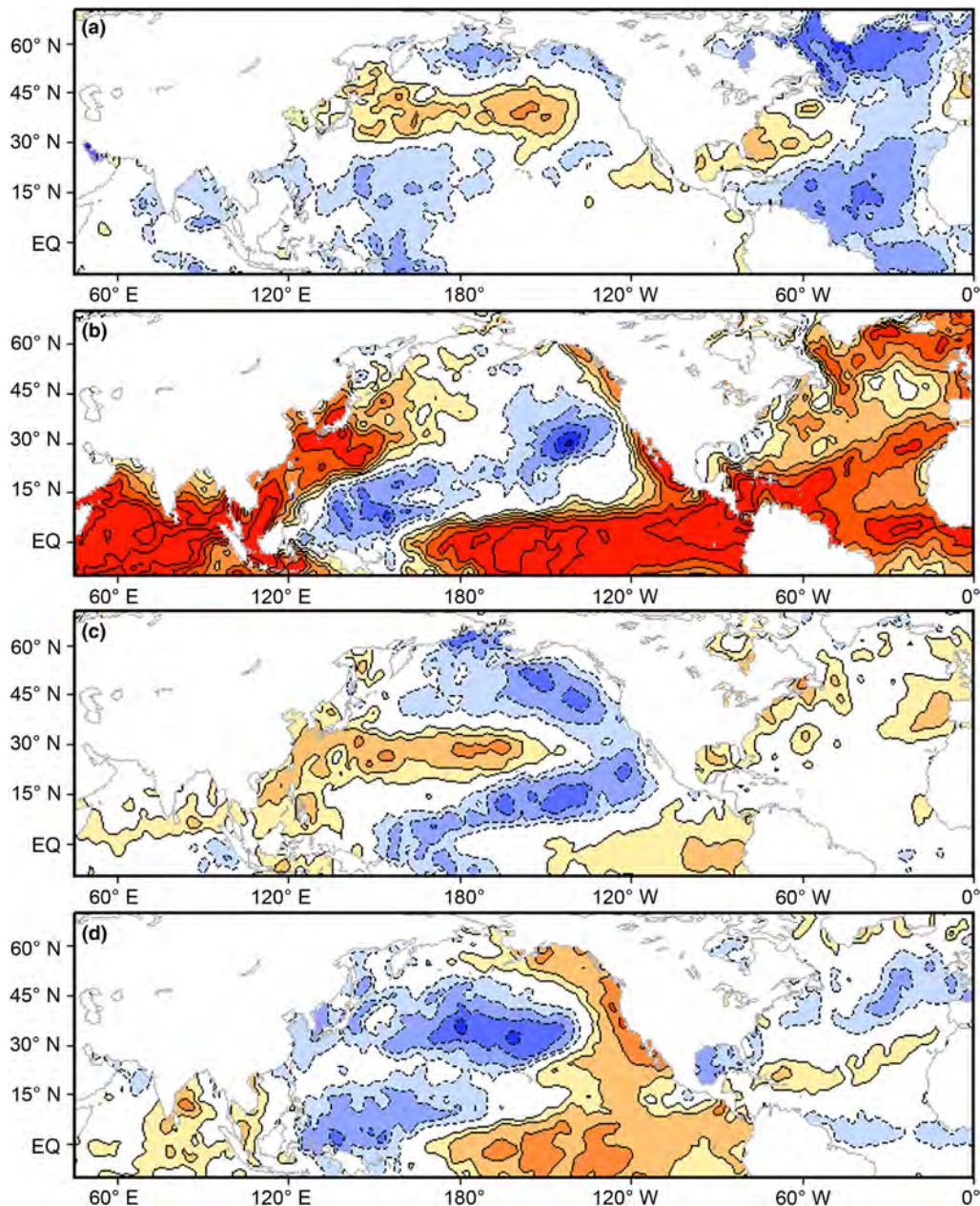


Figure 9 Correlation between the leading wintertime teleconnection patterns: (a) NAO, (b) ENSO related, (c) NPO/WP, (d) PNA, and SSA anomalies. Contour/shading interval is 0.1 m while the zero contour is suppressed. NAO, North Atlantic Oscillation; ENSO, El Niño-Southern Oscillation; NPO/WP, North Pacific Oscillation/West Pacific; PNA, Pacific-North America; SSA, sea surface temperature.

subseasonal-to-interannual climate research: ENSO, which is slowly varying and more predictable on seasonal timescales, explains relatively little hydroclimate variance in the Northern extratropics. The NAO, by contrast, explains more surface climate variance but is substantially less predictable.

Not surprisingly, the SST signature of the ENSO-related height pattern consists of large tropical correlations that resemble El Niño SSTs in the equatorial Pacific. Notable correlations are also present in the western Indian Ocean and the tropical and extratropical Atlantic. These include the well-documented ENSO links to warming of the adjacent basins, as well as capturing of more than just ENSO variability by this PC; including, possibly, the secular trend and multidecadal variability. The NPO/WP's SST correlations are not unlike NAO's Atlantic ones: a weak, tripolar, horseshoe-like structure in the extratropical basin; unlike NAO, however, it exhibits weak links with other basins.

The PNA SST correlations are broadly similar to the NPO's – an SST tongue extending from Japan into the midlatitude Pacific, surrounded by opposite-signed SSTs along the North American coast from the Aleutians to Baja Peninsula – but somewhat stronger, especially in the deep Tropics. A helpful distinction is the placement of the coastal anomalies: the off-coastal maximum in NPO/WP vis-à-vis the coastal maximum in PNA. The SST correlations of all three Pacific height patterns likely contain elements of the ENSO and Pacific decadal SST variability patterns, in view of the potential aliasing of SST variability due to the short analysis period (1979–2008) and the atmospheric-only nature of the PCA. An RPCA analysis of the combined variability of upper-tropospheric geopotential height and SST in a longer record minimizes such aliasing; see [Nigam \(2003\)](#) for more information.

The PNA SST correlations extend into the equatorial Pacific ([Figure 9\(d\)](#)), as noted above. This pattern was once thought to be the extratropical atmosphere's response to El Niño because of such correlations, despite the dominant intra-seasonal timescales of its PC (or teleconnection index) and the modest correlation (0.3 ~ 0.4) of the latter with the Niño 3.4 SST index. The potential aliasing of SST variability, noted above, led to PNA's spurious linkage with tropical SSTs: The PNA PC from the combined analysis of 200-hPa geopotential height and SST variations is correlated with the Niño 3.4 SST index at only 0.07.

The contemporaneous SST correlations of the recurrent 200-hPa height variability patterns raise the interesting question of cause and effect: Are the height patterns forced by the underlying SST patterns, or vice versa? The answer to this question is, unfortunately, complex as it is dependent on both the basin region and the variability pattern. Generally speaking, SST variations in the deep Tropics (e.g., ENSO related) are influential on the atmosphere on monthly timescales whereas variations in the middle–high latitude basins are the response. Consider the NAO: In the displayed phase (positive), the SLP pattern ([Figure 4\(c\)](#)) strengthens both the Icelandic Low and Azores High along with a northward displacement of the jet stream and storm track. This will result in anomalous westerly wind stress on the ocean northward of the climatological jet position, leading to increased vertical mixing and latent heat flux, and thus cooling of the surface

layer. The opposite arguments apply in the region off the US coast, where SSTs are warmer. The strengthened Azores High is, likewise, associated with stronger trade winds in the tropical Atlantic, leading to more upwelling and mixing off the African coast, and thus colder SSTs. As noted earlier, the influence direction is dependent on the basin region and variability timescales. The extratropical oceans can be influential on longer timescales and even on subseasonal ones through their preconditioning role. Clearly, this is an active research area in climate science requiring the use of advanced modeling techniques.

Northern Summer Teleconnections from RPCA

The Northern summer stationary waves are considerably weaker than the winter ones because of the weaker and northward displaced jet (and storm track). The summer regime thus consists of monsoonal circulations and only modest stationary Rossby wave propagation. For these reasons, the winter anomalies have been the target of most teleconnection analyses. The structure of recurrent height variability in Northern summer is however still of interest. A rotated EOF analysis (RPCA) of June, July, and August (JJA) 200-hPa geopotential height anomalies is conducted in a fashion similar to the wintertime analysis except for the analysis domain. The domain used in the summer analysis is restricted to 20–90° N. This change is made to emphasize the extratropical modes; inclusion of the Tropics leads to a noisier analysis.

The summer results are displayed in [Figure 10](#). The leading patterns are, perhaps, relatable to the winter patterns. The first one is labeled NPO/WP due to the presence of a north–south dipole over the North Pacific near the date-line. The second one is referred as the NAO on account of the dipole over the northeastern Atlantic. An ENSO-related pattern or a PNA look-alike was not identified. The third leading pattern exhibits higher geopotential heights in the global Tropics and a coherent ridge over the western sub-Arctic. The first four modes explain less variance than in winter, indicating the more disorganized structure of summertime variability. Notice that even the patterns resembling NPO/WP and NAO are more regionally confined, consistent with brief remarks on reduced Rossby wave activity in Northern summer; see [Folland et al. \(2009\)](#) for more discussion of the summer NAO, the most studied summer teleconnection.

Southern Winter Teleconnections from RPCA

The very different distribution of continents and mountains in the Southern Hemisphere (SH) results in muted seasonality and stationary waves. The SH winter climatology is dominated by a strong polar vortex, and thus more zonally symmetric flow. The lack of continents and large mountain ranges lead to reduced orographic forcing and land–sea contrast, both resulting in diminished stationary Rossby wave activity. An RPCA analysis of the SH winter height variability is briefly discussed here. It is identical to the Northern winter

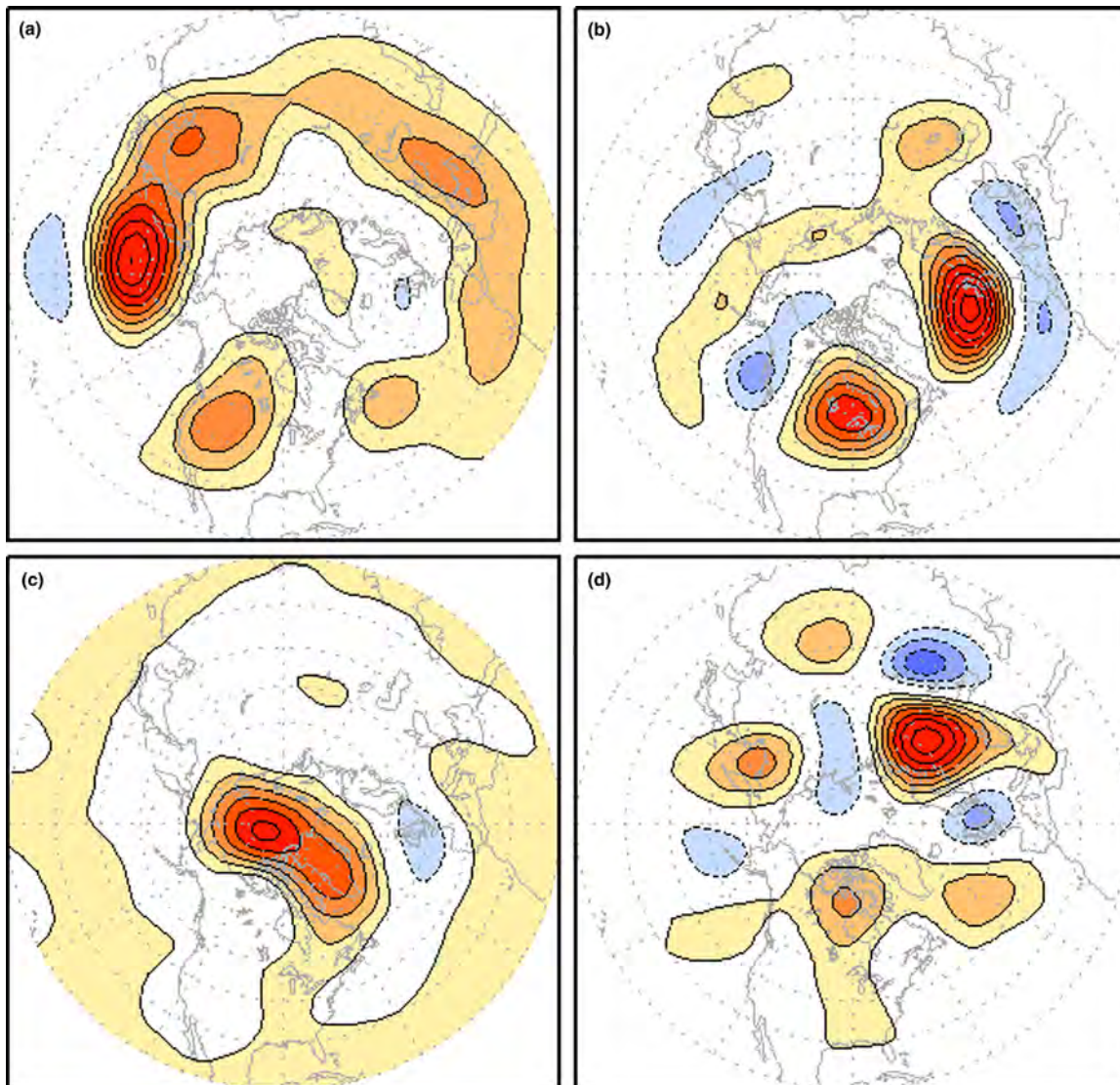


Figure 10 Four leading summertime (JJA) teleconnection patterns that emerge from a rotated EOF analysis of 200-mb geopotential height. The domain of the analysis is 20–90° N. Only the leading two modes, (a) and (b), are clearly identifiable as the NPO/WP and NAO, respectively. Contour/shading interval is 8 m; the zero contour is suppressed. Percentage of explained variance: (a) 11.9, (b) 8.5, (c) 8.0, (d) 7.4. JJA, June, July, August; EOF, empirical orthogonal function; NPO/WP, North Pacific Oscillation/West Pacific; NAO, North Atlantic Oscillation.

analysis: the domain includes the Tropics (30° N–90° S), and the eight leading patterns are rotated using the varimax criterion.

The four leading patterns are shown in [Figure 11](#). The first one is analogous to the NAO, but slightly more annular in nature. The larger amount of explained variance (~16.4%) relative to the other patterns indicates that SH variability is dominated by fluctuations of the polar vortex; not surprising, given the zonal nature of the SH circulation. Patterns 3–4 are more classic teleconnections: The third pattern consists of a strong center in the Bellingshausen Sea in the far South Pacific, surrounded by three weaker centers, while the fourth one is dominated by a wave-3 pattern around the pole. Patterns 1, 3, and 4 were identified in some form by [Mo and White \(1985\)](#), the first analysis of SH

winter variability; see this study for more details on SH teleconnections.

For reference, [Figures 12–14](#) show the surface temperature and precipitation footprints of select winter patterns of SH height variability; in the interest of space, only a few prominent features are noted below. Because of its polar domain, the first pattern has weak temperature and precipitation footprint over the inhabited continents. Pattern 2 ([Figure 12](#)) is linked with wide-spread warming of the Tropics, and more precipitation over Amazonia and southern South Africa, and a precipitation dipole over Australia (dry to the east, wet in the north); some of these signals are well documented in the literature as El Niño's SH winter impact. Pattern 3's precipitation impact is weak but it is linked to a prominent north-south temperature dipole over South America ([Figure 13](#)).

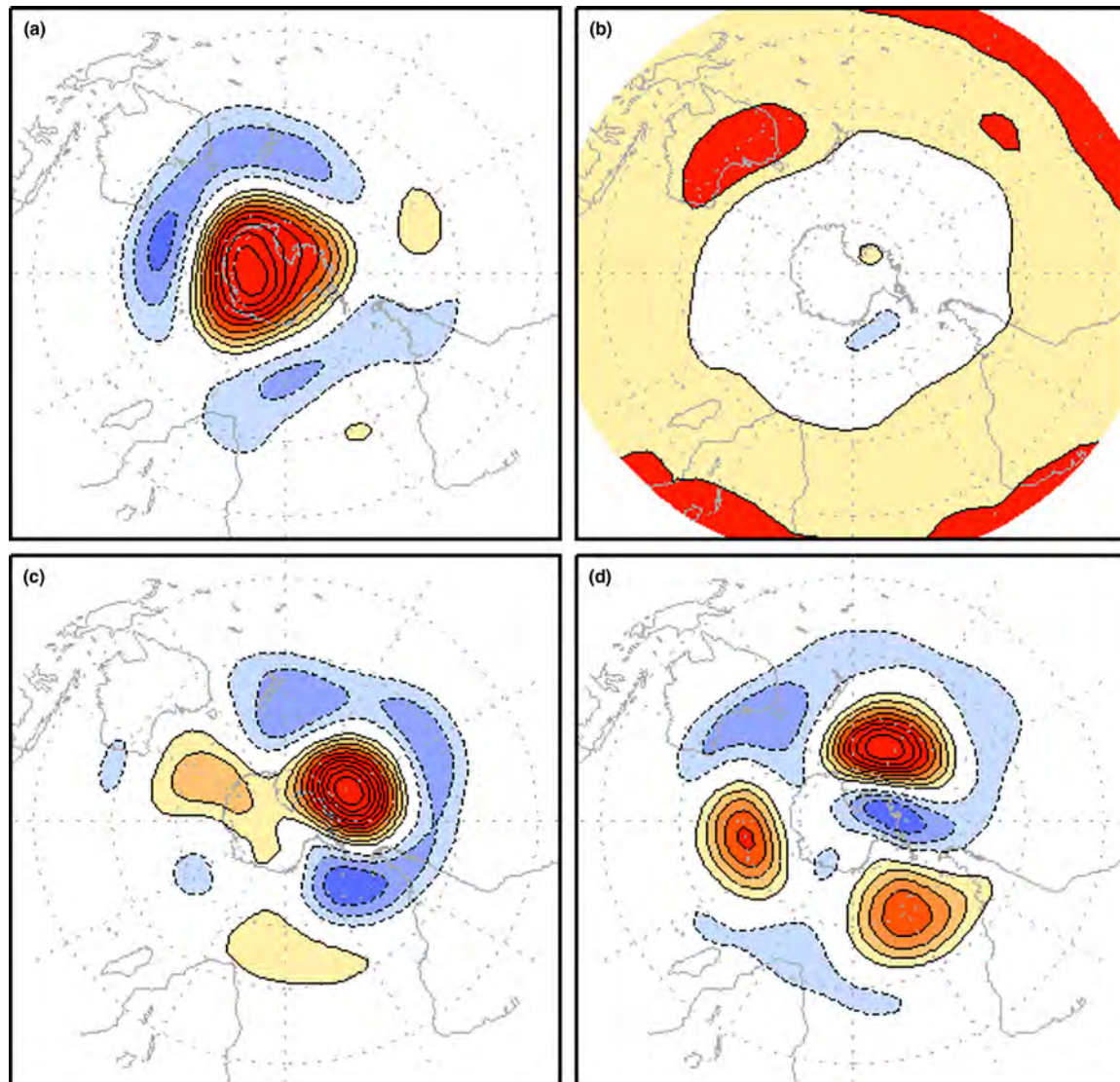


Figure 11 The leading patterns that emerge from a rotated EOF analysis of 200-mb height in SH wintertime (JJA). The domain used is 30° N– 90° S. The contour interval is 10 m while the zero contour is suppressed. Panels (a)–(d) represent patterns 1–4. Percentage of explained variance: (a) 16.4, (b) 11.9, (c) 11.5, (d) 10.4. JJA, June, July, August; EOF, empirical orthogonal function; SH, Southern Hemisphere.

Although not expected from the height anomaly structure, mode 4 exerts substantial impact over Australia (Figure 14), with wet anomalies everywhere except the southeastern region.

Annular Modes

Closely related to teleconnections are the annular modes, which have received considerable attention in recent years. While teleconnections are the climate links between geographically separated regions, the annular modes represent the seesaw (i.e., out-of-phase links) between the poles and the surrounding midlatitudes; annular modes can be viewed as the teleconnections of the polar region. The annular mode in the NH and SH is referred as the Arctic Oscillation and

Antarctic Oscillation (AO and AAO), respectively. The annular pattern is obtained from EOF analysis of the monthly 1000-hPa geopotential height anomalies (700 hPa for SH) poleward of 20° for the entire year. Key differences from the previous RPCA analysis are the lack of rotation of the PCs and the search for recurrent patterns among all calendar month (and not just winter) anomalies. Note, unrotated analyses often generate more spatially extended patterns in order to maximize the explanation of variance, as seen in Figure 15, which also shows the temperature and precipitation impacts of the annular patterns. Note, ‘annular pattern’ rather than ‘annular mode’ is, perhaps, more reasonable terminology as only spatial (and not spatiotemporal) variability is analyzed for their extraction.

The annular modes bear close resemblance to the leading mode extracted from RPCA of 200-hPa heights in each

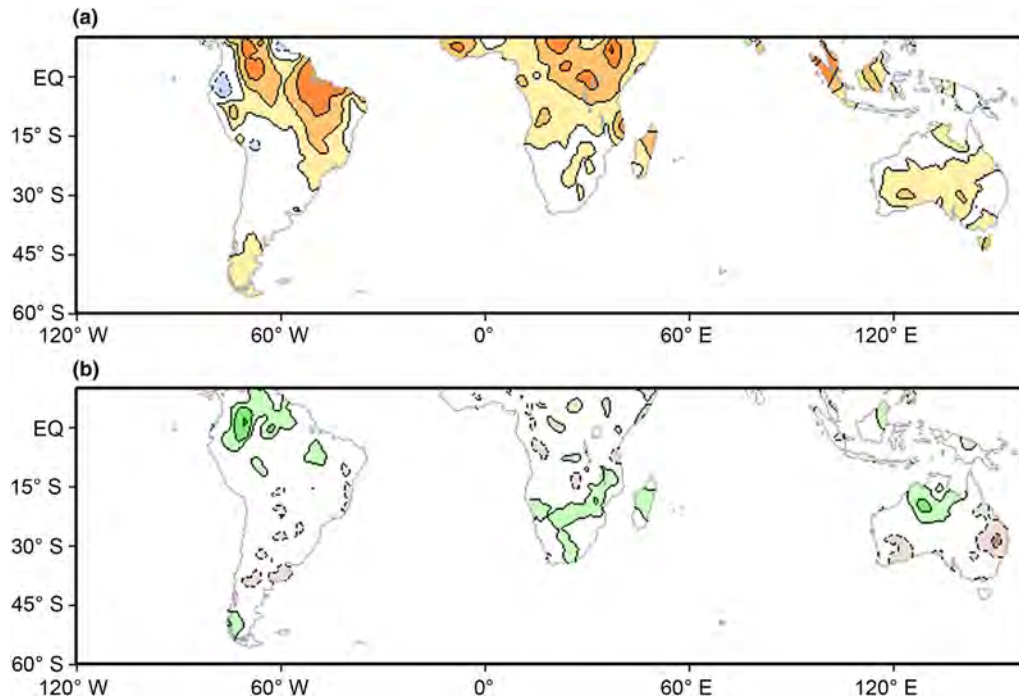


Figure 12 Same as in [Figure 3](#), except for the SH pattern 2. This is likely related to ENSO. ENSO, El Niño-Southern Oscillation; SH, Southern Hemisphere.

hemisphere. The AO has a stronger, coherent center of action in the Aleutians in addition to the essential elements of the NAO pattern. Not surprisingly, AO's year-round temperature and precipitation impacts are very similar to the winter impacts of the NAO (cf [Figure 4](#)). The close similarity of AO and NAO has led many to question whether the NAO is merely a region manifestation of the larger-scale annular mode (AO). It is noteworthy that neither the AO nor AAO are

strikingly annular; especially the AO. The AO footprint in the lower stratosphere (not shown) however appears substantially more annular; as does the NAO footprint (cf [Figure 8\(c\)](#)).

Subseasonal Tropical Variability – MJO

The ENSO-related pattern reveals one way in which the Tropics can influence the extratropics: An interannual shift in the preferred area of tropical convection/precipitation leads to anomalous divergent motions, which generate a Rossby wave source that, in turn, alters midlatitude storm tracks and extratropical climate. Zonal variations in tropical convection occur on timescales other than interannual ones as well: The MJO – representing convection variability in the tropical Indian Ocean and Western Pacific basins on 30- to 50-day timescales – can, like ENSO, influence the climate in the extratropics, albeit on subseasonal timescales.

When the MJO is active, convection is enhanced over the eastern Indian Ocean at the expense of the West Pacific. This generates an anomalous divergent circulation that leads to retraction of the East Asian jet. The jet retraction and related modulation of storm tracks influence the circulation and hydroclimate over the North Pacific and North American regions; for example, weaker Aleutian Low and higher than normal heights over eastern North America. These MJO influences can implicitly influence the NAO and PNA structure, but only modestly as these teleconnection patterns are robustly manifest in the MJO-filtered data as well.

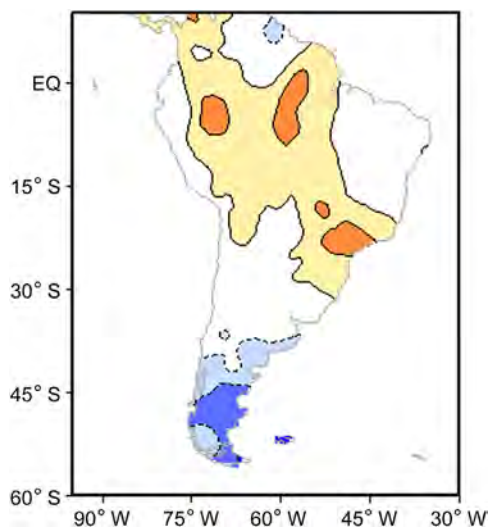


Figure 13 Similar to [Figure 12](#), except only showing the South American temperature footprint for pattern 3.

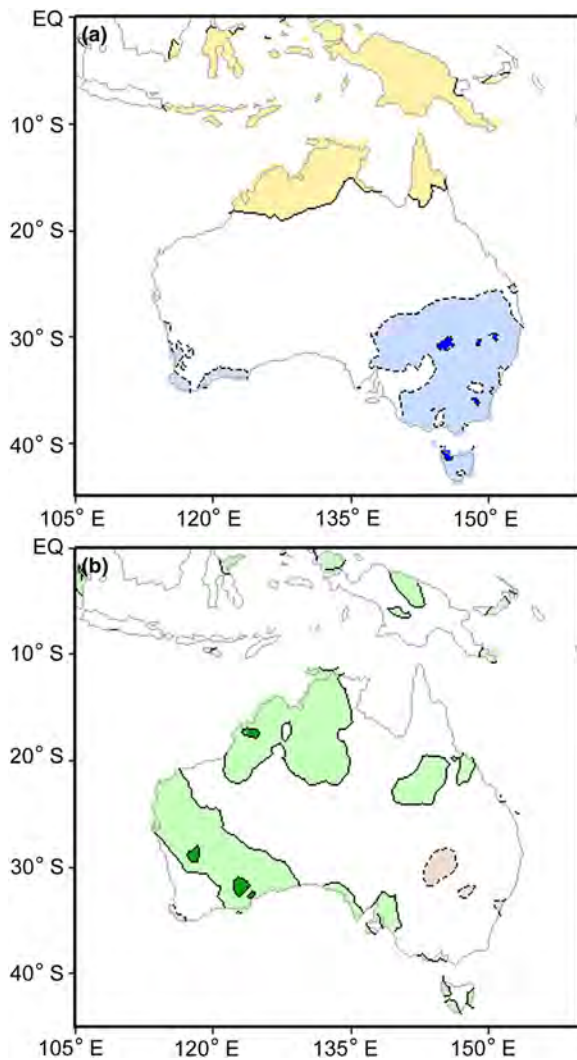


Figure 14 Similar to [Figure 12](#), except the temperature (a) and precipitation (b) footprints are shown only over Australia for pattern 4.

Subseasonal Teleconnection Analysis

Climate teleconnections, discussed above, were obtained from the analysis of monthly averaged anomalies, using techniques keyed to an optimal accounting of the temporal variance. These attributes steered the analysis toward extraction of the mature phase of the leading teleconnection patterns. Monthly averaging filtered the large-scale synoptic waves in the troposphere and facilitated focus on the 'standing' component of low-frequency variability. A month is not too long a period in context of large-scale ocean-atmosphere interaction, but it is an extended averaging period in context of the dynamical and thermodynamical processes generating climate teleconnections. These processes evolve rapidly – on pentad-to-weekly timescales – and their resolution is critical for the description of the nascent-to-mature and decay phases of the teleconnection patterns, and for advancing understanding of the excitation mechanisms. Insights into the evolution of teleconnection

patterns can advance the subseasonal prediction of the climate system.

In the following, the submonthly evolution of PNA variability is briefly discussed to illustrate an interesting line of contemporary teleconnection research. The PNA pattern is chosen as its evolution was described earlier from a simpler (and less accurate) analysis ([Nigam, 2003](#)), facilitating assessment of the new analysis strategy. The CFSR, used earlier at monthly resolution, is analyzed at pentad (5-day average) resolution in this section. The analysis period covers 30 extended winter (November–March) seasons from 1979 to 2008, and the 200-hPa geopotential height anomalies are analyzed, as before. To emphasize pattern development and decay, a technique called *extended EOF analysis* is used. Extended EOF analysis is a powerful spatiotemporal analysis technique, but one that can be easily implemented using the standard EOF analysis infrastructure; by substituting a contiguous *series* (e.g., from $T - 2$ to $T + 2$ time steps) of anomaly patterns in place of the contemporaneous one (i.e., $T = 0$). The leading variability mode in this case is not a single spatial pattern but the most recurrent temporal series of spatial patterns, or the most recurrent spatiotemporal pattern. In this illustrative example, a 5-pentad window is chosen ($T - 2$ to $T + 2$ pentads). The seven leading modes are rotated using the varimax criterion to allow for more spatial discrimination.

The leading mode from this spatiotemporal analysis represents the development and decay of the NAO (not shown). The fourth leading mode is closely related to the PNA; a 5-pentad evolution is shown in [Figure 16](#). An interesting finding here is that the development and decay of the PNA is associated with westward progression of height anomalies across the high latitudes. At $T = -3$, there is a notable height center in the NAO region of the North Atlantic. It is thus not surprising that there is a small but significant lag correlation between modes one and four ($r = -0.35$), with the negative NAO *leading* the positive-phase PNA pattern. The retrogression of the northern height anomalies is consistent with the advection of planetary vorticity, but cannot adequately explain the development of the robust anomaly center south of the Aleutians.

To help set forth a plausible basis for the NAO–PNA link, the impact of the NAO on the meridional wind is assessed; meridional winds highlight the shorter zonal scales of the midlatitude quasi-geostrophic flow, and thus the zonal propagation of stationary Rossby waves. [Figure 17\(a\)](#) shows contemporaneous regressions of the PC associated with the positive NAO pattern onto the 200-hPa meridional wind, along with the climatological winter position of the East Asian jet. The NAO apparently forces a wave pattern in the subtropics between East Africa and southern Asia that culminates in the North Pacific. [Figure 17\(b\)](#) shows the 2-pentad lag regression of the same NAO PC onto the 200-hPa zonal winds. The result is a subtle retraction of the East Asian jet, consistent with the negative-phase PNA pattern.

The analysis presented above serves to illustrate the nature of contemporary research in climate teleconnections rather than definitive findings on PNA evolution; durable and corroborated findings on teleconnection evolution have yet to

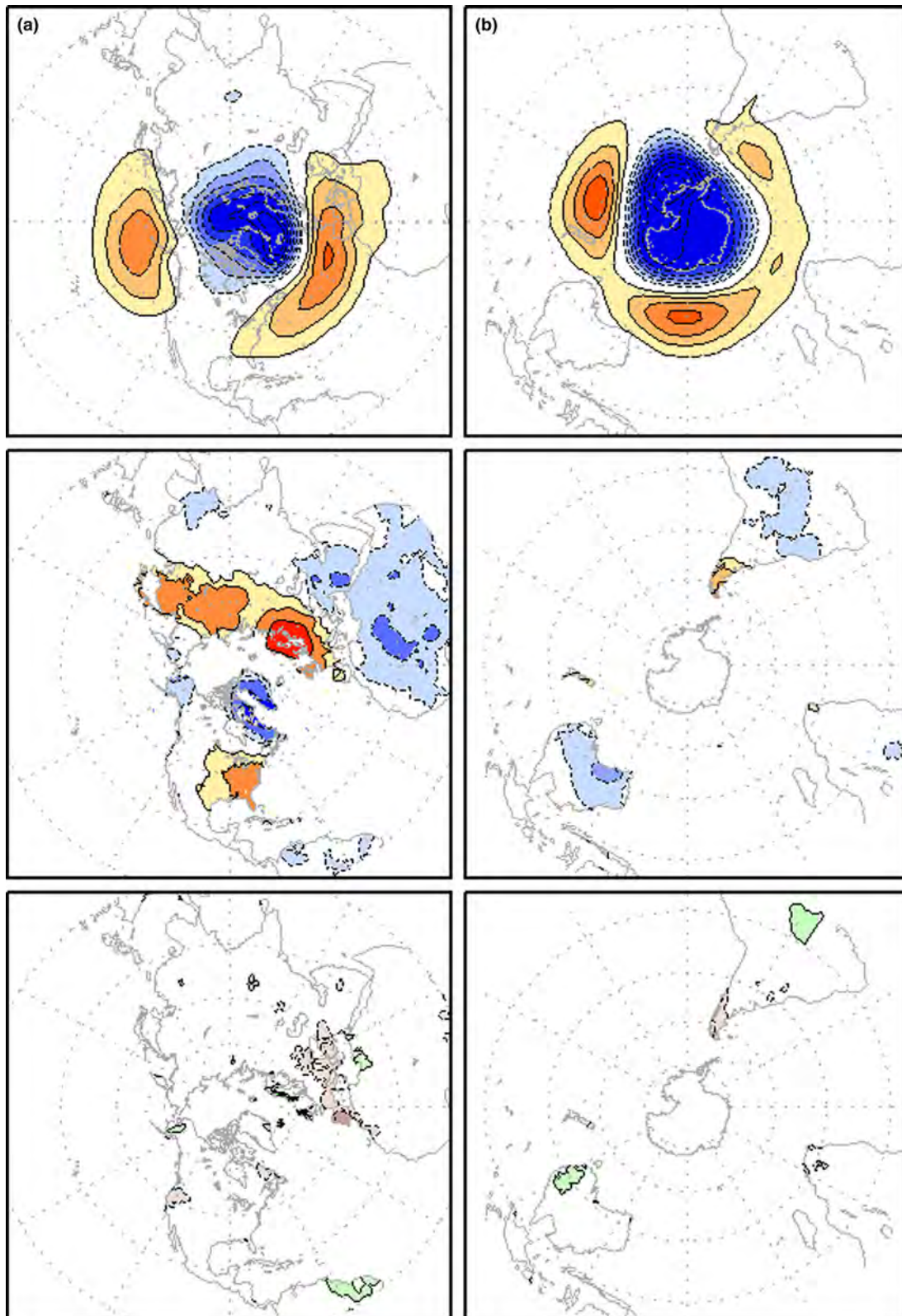


Figure 15 The two annular modes, (a) the Arctic Oscillation and (b) the Antarctic Oscillation (AAO), are shown along with their temperature and precipitation footprints. Annular modes are calculated as the leading EOF of 1000-mb geopotential height (700-mb geopotential height for AAO). Note that the entire year is used to calculate the pattern. Contour interval for the height patterns is 5 m. Hydroclimate footprints are shown as correlations between the principal components and CRU temperature and precipitation, contoured at 0.15 intervals. For all panels, the zero contour is suppressed. EOF, empirical orthogonal function.

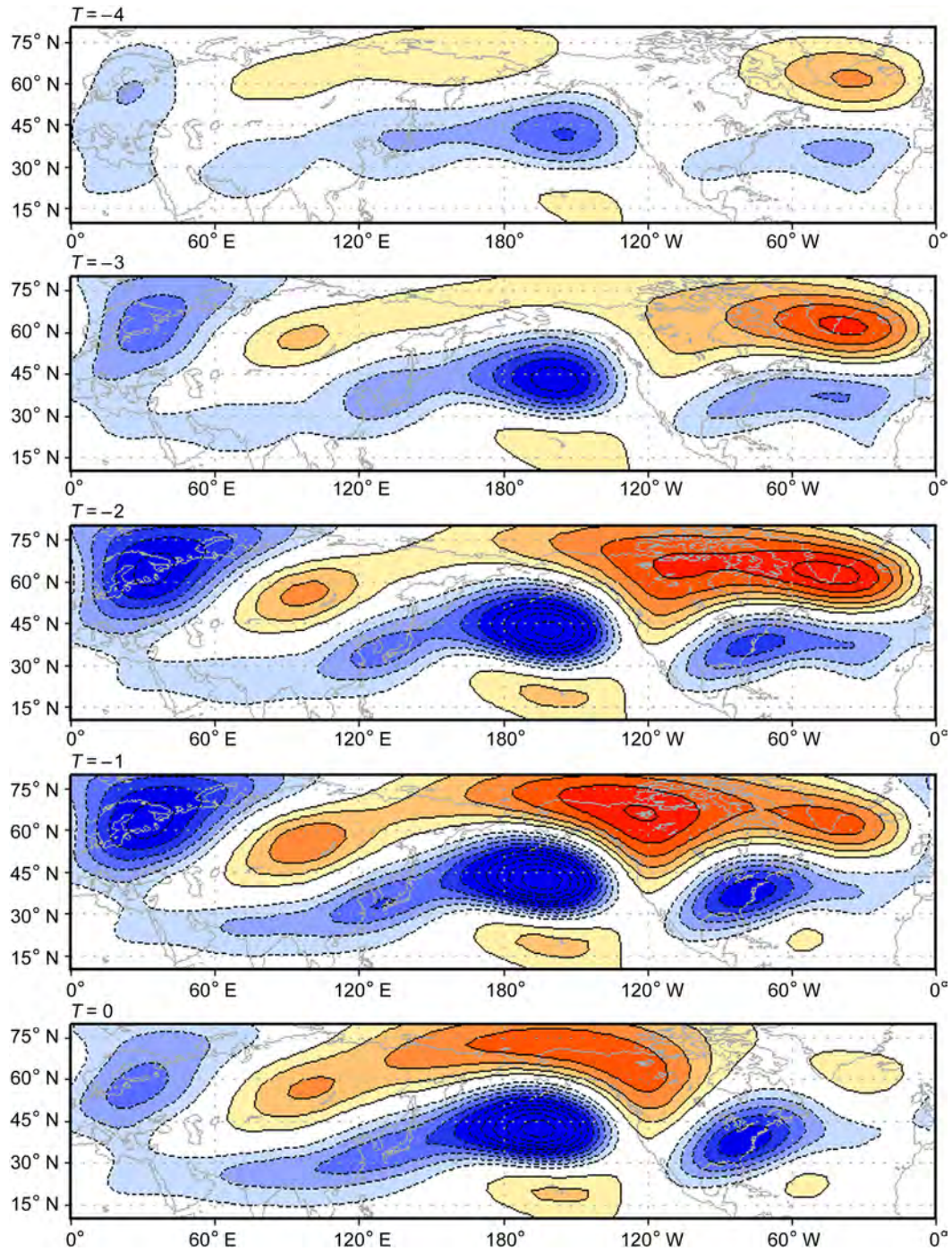


Figure 16 The fourth leading mode from a rotated, extended EOF analysis on extended winter 200-hPa height at pentad resolution. This mode closely resembles the PNA. The figure is presented as the lead/lag regression ($T = -4$ to $T = 0$) of the PC onto the height field. The contour interval is 10 m and the zero contour is suppressed. EOF, empirical orthogonal function; PNA, Pacific–North America; PC, principal component.

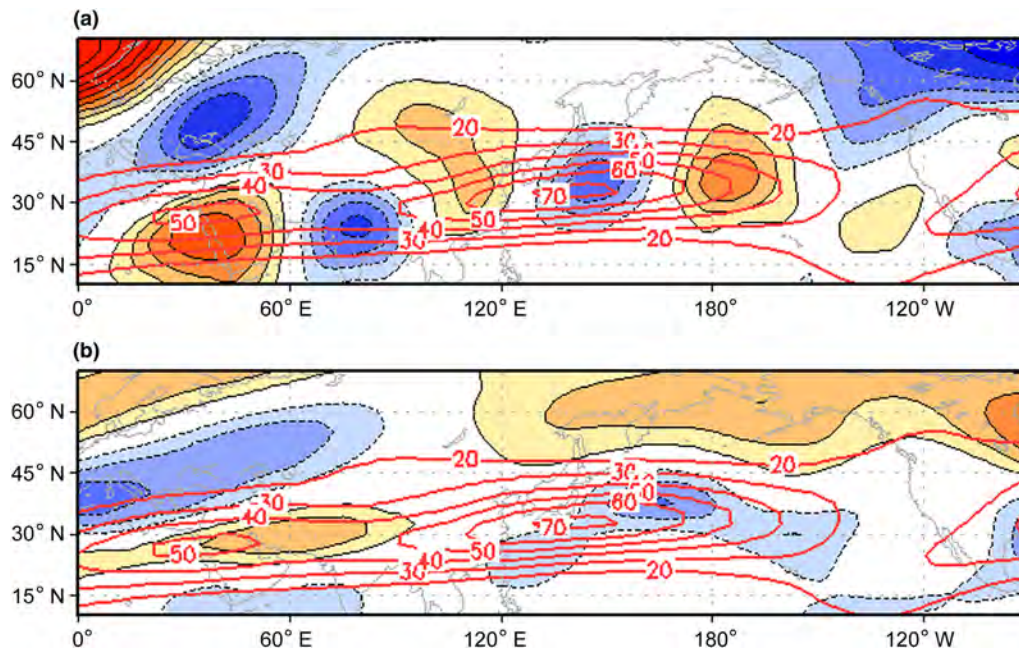


Figure 17 (a) The contemporaneous regression of the leading PC (NAO) onto 200-hPa meridional wind is contoured/shaded at 0.5 m s^{-1} intervals. The zero contour is suppressed. Bold red contours show the winter climatology of the 200-hPa zonal wind at 10 m s^{-1} intervals. (b) The 2-pentad lag regression of the leading PC (NAO) onto the 200-hPa zonal wind field is contoured/shaded at 1 m s^{-1} intervals with the zero contour suppressed. As in (a), bold red contours represent the winter jet climatology. NAO, North Atlantic Oscillation; PC, principal component.

emerge. The recent focus on submonthly climate prediction has however spurred climate scientists to investigate the development and decay of the leading winter teleconnection patterns.

See also: **Climate and Climate Change:** Climate Variability: Seasonal and Interannual Variability. **Dynamical Meteorology:** Rossby Waves; Stationary Waves (Orographic and Thermally Forced). **Stratosphere/Troposphere Exchange and Structure:** Global Aspects. **Tropical Meteorology and Climate:** Madden-Julian Oscillation: Skeleton and Conceptual Models.

- Folland, C.K., Knight, J., Linderholm, H.W., Fereday, D., Ineson, S., Hurrell, J.W., 2009. The summer North Atlantic Oscillation: past, present, and future. *Journal of Climate* 22, 1082–1103.
- Mo, K.C., White, G.H., 1985. Teleconnections in the southern hemisphere. *Monthly Weather Review* 113, 22–37.
- Nigam, S., 2003. Teleconnections. In: Holton, J.R., Pyle, J.A., Curry, J.A. (Eds.), *Encyclopedia of Atmospheric Sciences*. Academic Press, Elsevier Science, London, pp. 2243–2269.
- van den Dool, H.M., Saha, S., Johansson, Å., 2000. Empirical orthogonal teleconnections. *Journal of Climate* 13, 1421–1435.
- Wallace, J.M., Gutzler, D.S., 1981. Teleconnections in the geopotential height field during the northern hemisphere winter. *Monthly Weather Review* 109, 784–812.

Further Reading

- Barnston, A.G., Livezey, R.E., 1987. Classification, seasonality and persistence of low-frequency atmospheric circulation patterns. *Monthly Weather Review* 115, 1083–1126.